International Journal of Advanced Robotic Systems

OPEN ACCESS ARTICLE

Development of a Minimally Actuated Jumping-Rolling Robot

Regular Paper

Thanhtam Ho[1] and Sangyoon Lee[1]*

1 Konkuk University, Seoul, Republic of Korea
*Corresponding author(s) E-mail: slee@konkuk.ac.kr

Received 05 September 2014; Accepted 22 January 2015

DOI: 10.5772/60495

Abstract

This paper presents development of a hybrid mobile robot in order to take advantage of both rolling and jumping locomotion on the ground. According to the unique design of the mechanism, the robot is able to execute both jumping and rolling skilfully by using only one DC motor. Changing the centre of gravity enables rolling of the robot and storage of energy is utilized for jumping. Mechanism design and control logic are validated by computer simulation. Simulation results show that the robot can jump nearly 1.3 times its diameter and roll at the speed of 3.3 times its diameter per second.

Keywords hybrid mobile robot, jumping robot, rolling robot

1. Introduction

Various efforts to enable a mobile robot to achieve multiple modes of locomotion have been reported. One useful choice for ground robots is a combination of rolling and jumping. Rolling locomotion possesses the advantage of travel speed, especially on hard and flat surfaces [1]. It is also considered energy-efficient, because a rolling robot does not need to expend energy lifting up its body for movement [2, 3]. On the other hand, jumping can be considered as a better way for ground robots to avoid obstacles [2]. It is reported that some robots are able to jump ten times as high as their body heights [4, 5]. However jumping requires a great deal of energy for a very short time period.

Reference [6] introduces an example of robots that employ both jumping and rolling. Although the robot can execute both locomotion types, overall performance is not considered remarkable. The spherical robot with 300 mm diameter can jump up to 0.6 times its height but it has weak ability in rolling. The robot presented in [7, 8] is another example where wheeling and jumping are integrated. The robot is quite skilful in both jumping and wheeling. The robot, with 40 mm diameter, can jump up to 100 mm and run at 310 mm/sec. This robot can also easily steer to change the direction of movement. Complexity in the structure is a disadvantage of the robot, which is due to many actuators. Another disadvantage is found in the robot's jumping mechanism. The mechanism includes a small tip spring that requires a rigid contact surface, and hence it may not work properly on soft surfaces. A shape-memory-alloy (SMA)-actuated crawling-jumping robot is reported in [9]. The robot uses SMA as an actuator and employs the deformation principle for rolling. This work suggests a way of using unconventional actuators for hybrid mobile robots.

Although incorporating multiple modes of locomotion in one robot can increase its manoeuvrability, it can also cause

decreased energy efficiency. This is because the number of actuators on a robot is larger than or equal to the number of locomotion gaits. Increase of the number of actuators usually leads to increase of weight, size, and complexity. This paper presents development of a robot that can locomote by means of jumping and rolling using only one actuator. The proposed robot is designed to be able to perform both modes of locomotion by using only one DC motor. Simplification ideas in the design achieve the ability with high efficiency.

2. Robot Design

This section describes principles of rolling and jumping and explains how they are converted into mechanism design.

2.1 Rolling Principle and Mechanism Design

The rolling principle of natural creatures has been studied and applied to the design of rolling mechanism. Though no biological creature with wheels exists, some can roll. According to the power source for rolling, rolling locomotion can be divided into two types: externally activated rolling and internally activated rolling. Rolling animals of the first type can roll with activation of external power, which is mostly gravity. Usually this method is used for escaping from danger rather than for travelling. The second rolling method is found in animals more frequently and is enabled by their own actuation system.

One of the most representative examples of passive rolling in nature is the Golden Wheel spider. Though the spider uses walking and running for the main mode of locomotion, it shows a different behaviour in order to escape from enemies: running first to the edge of a sand dune, rearranging its legs and forming a wheel shape to freely roll under gravity [10]. The rolling speed can be up to 1 m/sec.

The caterpillar of the mother-of-pearl moth, *Pleurotya ruralis*, uses rolling actively for locomotion [11, 12]. The caterpillar consists of 13 segments and legs are attached to each segment. The caterpillar may walk forward or even backward using the legs. During walking, the body segments form a hump or wave, which moves along the back. In a special case, the segment can coil up into a wheel and the caterpillar rolls by its wave momentum. The rolling speed and distance depend on the rolling surface, but the caterpillar can roll up to five revolutions with a travel speed of 40 cm/sec.

The advantages and rolling principles of both passive and active rolling creatures in nature provide inspiration for the design of the proposed rolling-jumping robot. For design of the overall external shape of the robot, a circular shape is considered based on the appearance of the rolling caterpillar. A spherical cage has an advantage over a cylindrical one in terms of mobility. Because of symmetry, a spherical robot can change direction easily. On the other hand, a cylindrical shape is more suitable for maintaining direction, which is a very useful attribute for minimally actuated robots like the proposed robot.

As for the caterpillar's rolling, movement of the centre of gravity (COG) is found to play an important role. The same principle is applied to the proposed robot, i.e., generation of rolling by change of COG of the robot. However, the proposed robot has an advantage over the caterpillar: though the caterpillar can produce only up to five rolls in each operation, the robot can roll unlimitedly because the COG is continuously controlled.

Using a single actuator, the COG can be changed by either rotating a mass around a centre-line or sliding a mass along an axis. In the latter method, motion of the mass is limited to a short range along a linear direction. The linear motion can also be utilized to extend a spring for jumping, which is a significant help in the design of the minimally actuated jumping-rolling robot.

The rolling principle can be explained using Fig. 1. The robot cage has a circular shape from each side and contact between the robot and the ground is made at one point only. This allows the robot to move easily to change the COG. As shown in Fig. 1(a), the robot has a slider part which can slide along a rack to change the COG. The slider includes a DC motor with a pinion that is attached to the motor shaft. A gear is linked to the rack element that is fixed to the body case. The rack and pinion mechanism converts rotation of the motor to translation of the slider along the body.

One can also notice several limit points of the slider in Fig. 1(a). Point B is the highest position of the slider while L is the lowest one. In order to prevent the latch from being locked to the hook during rolling, motion of the slider is limited to the range A-B instead of L-B. Point A is the lowest position at which the slider remains higher than the hook and is not locked to it. Range A-B is called the rolling range. Fig. 1(b) shows the model of the robot in rolling locomotion.

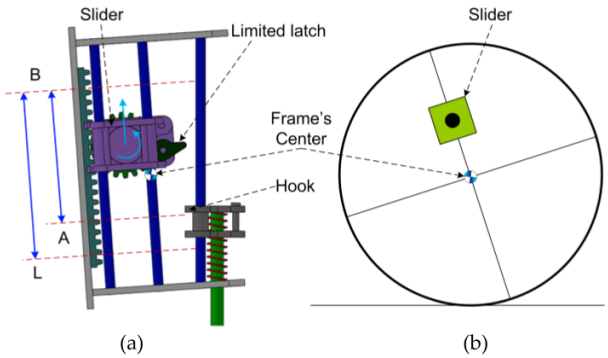

Figure 1. Rolling mechanism of the robot

Translation of the slider moves the COG of the entire robot body off the frame centre, which makes the robot roll as a result. It is obvious that if the slider lies on the right side of the safe zone, the robot will roll clockwise and vice versa. Thus, control of the position of the slider controls the rolling

motion. Fig. 2 illustrates the rolling motion of the robot determined by controlling the slider position.

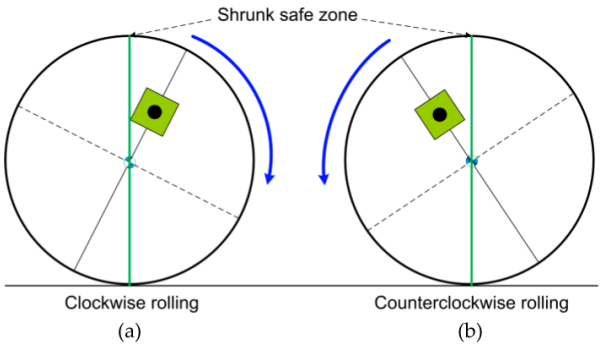

Figure 2. Control of rolling: (a) slider on the right side of the frame centre; (b) slider on the left side of the frame centre

2.2 Jumping Principle and Mechanism Design

Jumping of insects like the froghopper has previously been studied and applied to the design of jumping mechanisms. The jumping principle is strongly related to the question of how to employ an energy storage system. Compared to a directly activated jumping mechanism [13, 14], the jumping mechanism of insects like the froghopper shows significant advantages in terms of jumping distance and jumping height [15]. The energy generated by the muscles of the insect is gradually stored in a resilient device in the preparation phase and then released quickly to shoot the insect into the air in the jumping phase [16]. A mechanism to release the stored energy is equally important for such jumping structures. Since the proposed robot is actuated by only one actuator and the actuator works for an energy generator, a mechanism for energy release must work in a passive way.

The mechanism in Fig. 1 is also used for jumping, but it is used differently. The slider is designed to move between the highest position B and lowest position L in the jumping mode. The slider has a small element called the limited latch. The latch is designed especially for jumping. Another element used for the jumping mode is the hook. The hook is fixed to the leg and frame. In the rolling mode, the latch and the hook are kept separated and they do not have any function. In the jumping mode, the latch on the slider and the hook of the leg take an important role, allowing the energy generated by the DC motor to be stored in the spring. These two devices also act as the energy-releasing mechanism. The detailed structure of the slider is shown in Fig. 3.

In the design of the slider, the latch is linked to the support by a revolute joint. One torsion spring with low stiffness is inserted into the joint. The latch is called a limited latch because its rotation angle is restricted to the range of 0 to 90 degrees. One can see in the right-hand picture in Fig. 3 that the latch is obstructed by its support slate at the lower edge. This prevents the latch from moving further down-

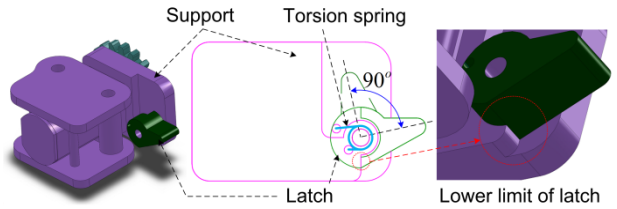

Figure 3. Structure of the slider and working of the latch

ward even if excessive force is applied. This configuration takes an important role in the jumping mechanism.

A shown in Fig. 4, the slider moves downward into the hook position for the start of jumping. Due to the pushing force of the hook, the latch rotates around its revolute joint. When the slider continues to move downward to the lowest position L, the latch loses contact with the hook and is rotated back to its original position by the torsion spring. This situation is illustrated in Fig. 4(a).

As noted in Fig. 4, the vector v_s represents the velocity of the slider with respect to the body base and v_b is the velocity vector of the body with respect to the lowest leg. This is a result, the latch becomes locked to the hook (see Fig. 4(b)),

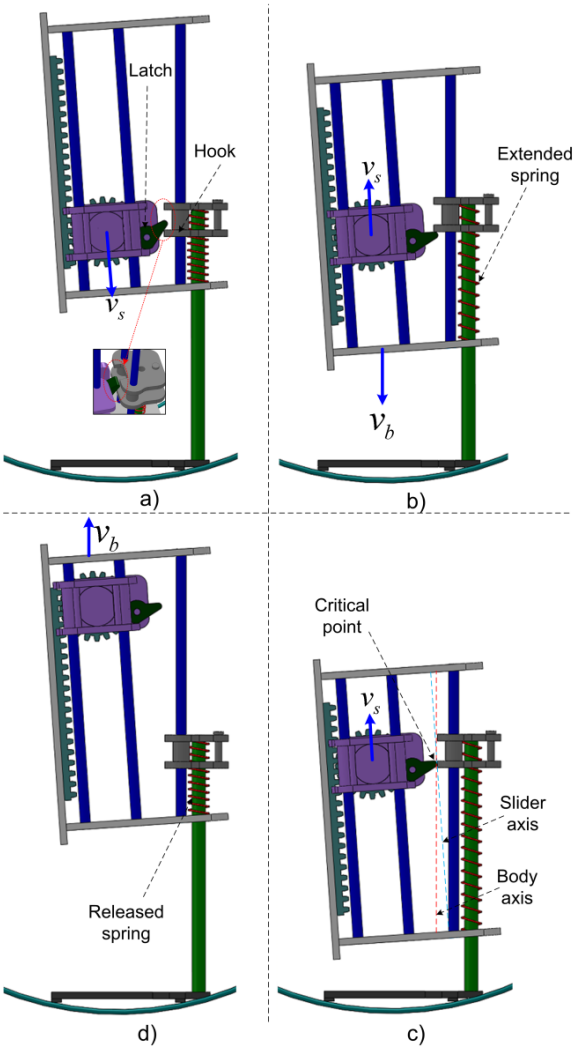

Figure 4. Sequence of jumping motion: (a) slider moving downward and being locked to the hook; (b) slider moving upward and extending the spring; (c) critical point where spring is maximally compressed and starting to release; (d) all the stored energy is released and the robot starts jumping

oscillation at the moment of landing. The rod is used as the pillar on which the body base hangs. The body base is linked to the rod by a prismatic joint. The main spring is connected along this joint. One terminal of the spring is attached to the hook and another is joined to the body base. Since the elastic force of the spring is much larger than the gravity of the robot body, nearly no translation occurs between the body and the rod, although the friction is quite small.

The major component of the slider is the DC motor, with a pinion attached to the shaft end. The DC motor is put on the support, to which a limited latch is attached. The slider may skid along the body base. Translation of the slider along the body is converted from rotation of the DC motor by the rack-and-pinion mechanism. One may note in Fig. 5 that the rack is a component fixed on the body base. Relative motion of the slider along the body base is the key factor to produce both rolling and jumping locomotion of the robot.

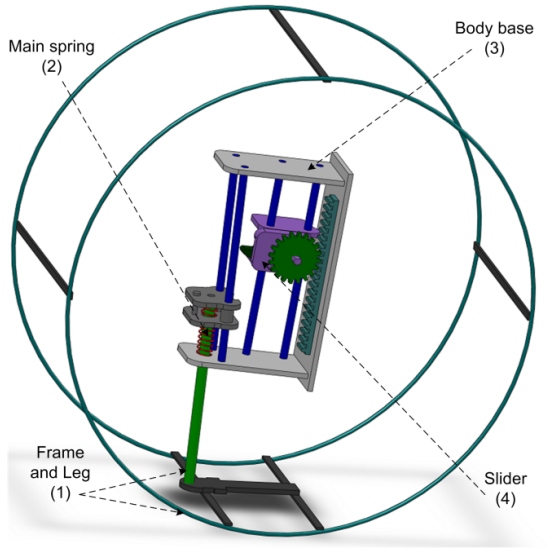

Figure 5. Overall design of the rolling-jumping robot with four major modules

3. Analysis and Computer Simulation

Rolling of the proposed robot is accomplished indirectly by the motion of the slider; therefore, control of rolling is much more difficult than control of wheeling or other locomotion. This section presents the rolling dynamics of the robot and a mathematical model. This model is also used to propose control logic of rolling, and is verified by simulation using Working Model and Matlab software. All analysis and simulation work is executed for a flat model on a hard-ground surface.

3.1 Analysis of Rolling Dynamics

A rolling model is developed assuming that the robot rolls on the ground without slipping. Since the robot is not able to move laterally, it can be simplified as a two-dimensional (2D) circular model. Fig. 6 shows the kinematics model of the robot in rolling and Table 1 shows all the parameters.

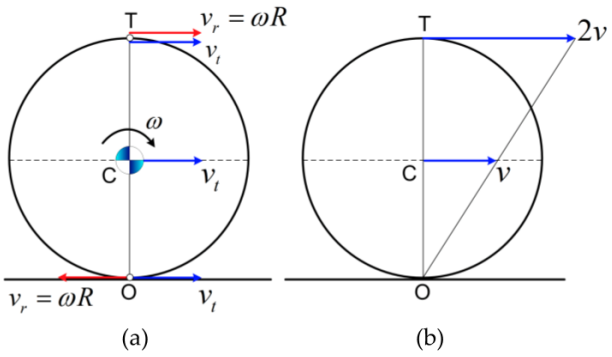

Figure 6. A model for rolling kinematics: (a) velocities at each point; (b) reduced model

As shown in Fig. 6(a), each point on the circle has different velocities. If v_O, v_C, and v_T are velocities at points O, C, and T, respectively, then they are computed as follows:

$$v_O = v_t - v_r = 0 \tag{1}$$

$$v_C = v_t = \omega R \tag{2}$$

$$v_T = v_t + v_r = 2\omega R = 2v_C \tag{3}$$

Symbol	Description
T	Top point of circular frame
C	Centre of circular frame
O	Contact point between frame and ground
R	Radius of circular frame
ω	Angular velocity
v_r	Velocity formed by rotational motion
v_t	Translation velocity

Table 1. Symbols of the kinematics model in Fig. 6

These computations imply that the velocity at T is twice as large as that at the centre C, while O is at rest instantaneously. Motion of the robot is equivalent to rotation with the instantaneous centre O (see Fig. 6(b)). Further, since O is the contact point between the circular frame and the ground, only static friction exists in this rolling motion.

The dynamics model of the rolling robot is displayed in Fig. 7 and parameters of the model are described in Table 2. Euler's equation is used to compute the rotational moments, while Newton's second law is utilized for translational components. If C is the temporary rotation centre for moment computation and I_{CM} is the moment of inertia of the whole robot with respect to the frame centre, one can obtain the following moment equation:

$$I_{CM}\ddot{\theta} = f_S R + m_2 g d\cos\theta \tag{4}$$

The total moment of inertia I_{CM} is the result of combining those of the frame, the body, and the slider. The frame is considered as a circular shape with a thin edge, and the moment of inertia of this part, I_F, is

$$I_F = m_F R^2$$

The body part has a rectangular shape with height H and width W. In the rolling mode, centroid of body is located at the frame centre, and its moment of inertia is as follows:

$$I_B = \frac{1}{12} m_B \left(H^2 + W^2\right)$$

The last component, the slider, is equivalent to a solid circle with radius r. One can calculate the moment of inertia for this part as

$$I_S = \frac{1}{2} m_S r^2$$

If the slider moves around the frame centre and the distance from the slider to the frame centre is d, the actual moment of inertia of the slider with respect to the frame centre can be obtained as follows using the parallel axis translation principle

$$I_S = \frac{1}{2} m_S r^2 + m_S d^2$$

Substitution of these parameters into equation of motion (4) leads to

$$I_{CM} = m_F R^2 + \frac{1}{12} m_B \left(H^2 + W^2\right) + \frac{1}{2} m_S r^2 + m_S d^2 \tag{5}$$

As for translation, applying Newton's second law, the equation of motion is written as follows:

$$f_S = -\left(m_F + m_B + m_S\right) a = -M_t \ddot{\theta} R \tag{6}$$

Here M_t is the total weight of the robot. From relation (4) and (6), equation of motion is rewritten as

$$\begin{aligned} &\left(m_F R^2 + \frac{1}{12} m_B \left(H^2 + W^2\right) + \frac{1}{2} m_S r^2 + m_S d^2\right)\ddot{\theta} \\ &= -M_t \ddot{\theta} R^2 + m_2 g d\cos\theta \end{aligned} \tag{7}$$

Note that parameters m_S and m_2 in (7) are identical to the mass of the slider. Therefore, (7) can be rewritten as

$$\begin{aligned} &\left(m_F R^2 + \frac{1}{12} m_B \left(H^2 + W^2\right) + \frac{1}{2} m_S r^2 + M_t R^2 + m_S d^2\right)\ddot{\theta} \\ &= m_S g d\cos\theta \end{aligned} \tag{8}$$

Equation (8) is the equation of motion of the rolling robot, in which displacement of the slider d is an input variable and rotation angle θ is an output quantity.

Firstly, the dynamics model is used for response analysis. A step function is selected as the input variable and slider displacement, rolling velocity, and rolling angle are recorded. By changing magnitude of the step input, output quantities are observed.

Fig. 8 shows the response of the system for three different cases. In all cases system parameters are kept the same except the magnitude of the step input. It is shown that when the step height increases, both magnitude and frequency of the rolling speed increase. For 10 mm step input, Fig 8 (a) shows that the rolling speed varies with a peak of 2.22 rad/sec and a frequency of 0.28 Hz.

In the case of 20 mm step input, the rolling speed increases to 3 rad/sec peak and vibrates at 0.4 Hz, as shown in Fig. 8(b). For 30 mm step input, the rolling speed reaches 3.8 rad/sec with 0.5 Hz. This result suggests that rolling speed of the robot can be controlled by changing the motion range of the slider.

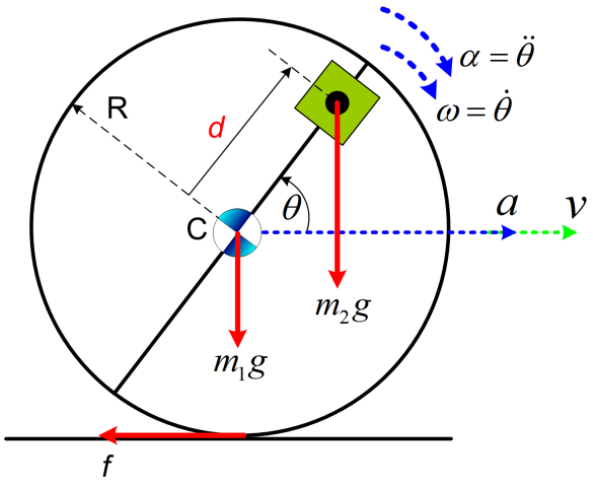

Figure 7. A model for rolling dynamics

Symbol	Description
θ	Tilt angle of robot body
α	Angular acceleration
v	Longitudinal velocity at circle centre
a	Longitudinal acceleration at circle centre
m_1	Mass of frame and robot body
m_2	Mass of slider
f_S	Static friction force
d	Displacement of slider

Table 2. Parameters of the rolling dynamics model in Fig. 7

The second test with the rolling dynamics model is done with control algorithms. The control algorithm is developed based on the rolling principle in Sec. 2. This means that the robot must keep the slider on the right side or in front of the circle centre in order to move forward. Here a feedback controller is used to adjust the slider position. The control rule is as follows:

$$u = K_C \cos\theta \tag{9}$$

In (9), cosθ indicates the relative position of the robot centreline with respective to a vertical line. This indicates whether the robot is leaning forward or not to move the slider to an appropriate position. The gain K_C represents the translation speed of the slider along the body axis. The test is performed for three cases, where K_C is 0.005, 0.01, and 0.02, respectively. Fig. 9 shows rolling results for K_C=0.02.

The test provides important results for controlling rolling motion. First, the results clarify the principle of rolling control. Forward rolling is obtained by keeping the slider position in front of the frame centre. As shown in Fig. 9, the rolling angle increases continuously without any ripple. In other words, the robot rolls forward smoothly.

Secondly, the results also illuminate the effect of the slider speed in relation to the rolling speed. By increasing feedback gain K_C, or slider speed, the rolling speed also increases dramatically. For example, when K_C is 0.005, the robot rolls up to 9 rad in 5 sec. In the same amount of time, when K_C increases to 0.02 the rolling angle also increases to 33 rad (see Fig. 9). This suggests that the slider speed can be utilized to control the rolling speed.

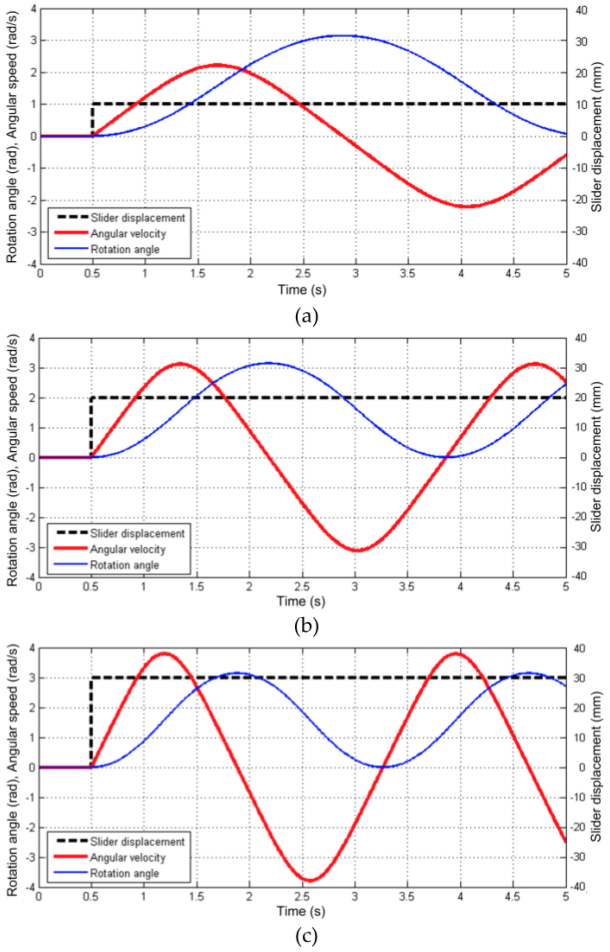

Figure 8. Step responses for rolling: (a) response with 10 mm step input; (b) response with 20 mm step input; (c) response with 30 mm step input

3.2 Computer Simulation of Rolling and Jumping

This section presents simulation work to verify the working of the robot mechanism and the control logic. Since only jumping and rolling motions in plane are introduced, motion in the lateral direction is neglected. Fig. 10 displays the equivalent 2D model of the robot that is developed for simulation. Working Model 2D (WM2D) is selected for the

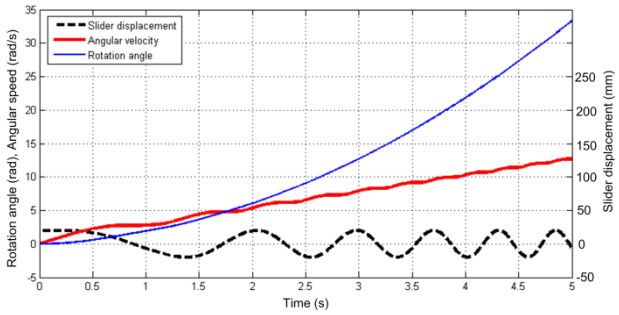

Figure 9. Example of forward motion control with feedback gain K_C=0.02

dynamics simulation. Control logic is implemented using Matlab software. In this co-simulation scheme, communication between two software packages is performed by the dynamics-data-exchange protocol (DDE).

The input data for the controllers are transferred from WM2D to Matlab software and the output from the controller in Matlab is sent to the DC motor model in WM2D. The design model presented in Section 2 is directly imported to WM2D to build the dynamics simulation model. The model parameters and the simulation conditions are summarized in Table 3.

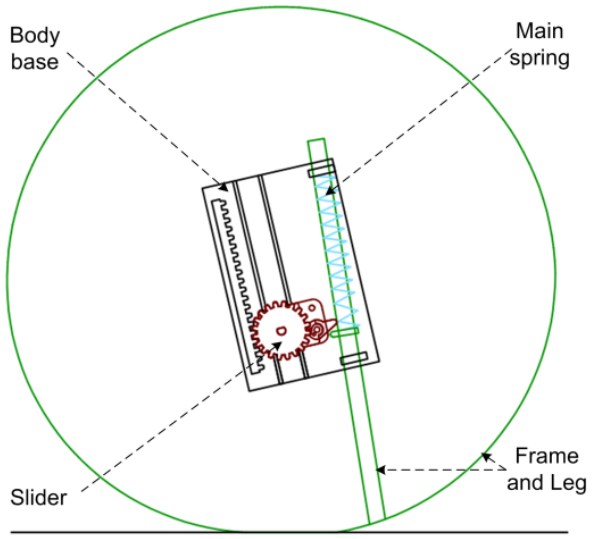

Figure 10. 2D simulation model

Unlike wheeled robots, where rotation of actuator is directly transferred to the wheels, the motion of a DC motor indirectly controls rolling and jumping in the proposed robot. A two-level control model is developed for the robot. The high-level controller receives a task from the user or is interfaced directly with the environment. It also makes decisions and gives commands to the low-level controller. The low-level controller adjusts rotation of the motor such that the robot can perform basic motions including forward and backward rolling, stopping, and jumping.

The low-level controller moves the slider along the rack in order to perform specific motions given by users. The control parameters for the low-level controller are the position and the motion speed of the robot. For example, the slider must be kept in front of the cylinder-frame centre for forward rolling. In simulation, a simple controller which combines several rules is utilized for this purpose.

Symbol	Description	Value
D	Diameter of the cylindrical frame	180 mm
m_f	Mass of the frame	12 g
m_b	Mass of the body	34 g
m_s	Mass of the slider	20 g
l_0	Spring displacement	50 mm
K	Spring stiffness	0.36 N/mm
φ_0	Initial tilt angle in jumping	10° - 25°
Γ	Skew angle between slider axis and body axis	3°
k_f	Friction coefficient between frame and ground	1.0

Table 3. Parameters of the simulation model in Fig. 10

Fig. 11 presents a flowchart of the control logic for forward motion. First, rolling speed (v) is measured and compared to desired speed (v_d). For this parameter a PID controller is used to set the speed of the DC motor, or the sliding speed of the slider. The tilt angle θ is measured to determine the posture of the robot's vertical axis. According to the tilt angle, the controller will adjust the slider position to keep the robot's COG in front of the frame centre with motor speed v_m.

The first simulation set is to evaluate jumping. The spring stiffness is kept at 0.36 N/mm while the tilt angle of the robot is changed from 10 to 25 degrees. Two low-level control algorithms for jumping and stopping are executed. Each jump takes about 1 sec; however, the time for recovering stability after each jump is about 4 sec. The jumping height and jumping distance are measured and summarized in Table 4.

The second simulation set was executed to verify the rolling motion. Here all basic motions employed by the low-level controller are executed in sequence. The rolling speed and the response time of the low-level controller are examined from this simulation. The effect of the slider speed on the rolling velocity is also evaluated. Fig. 12 shows angular velocity of the robot in the simulation.

The plot in Fig. 12 shows the average angular velocity of the robot in rolling. In this simulation, the compound motion is supervised by the high-level controller. From 1 sec to 5 sec, the robot is commanded to roll forward. Then, the rolling direction is reversed and the robot moves backward until 9 sec. Finally, the robot rolls forward again with slower velocity and stops at 13 sec. One can see from Fig. 12 that the robot performs rolling completely following given commands. Although it is hard to keep the instantaneous velocity constant, its average value is somewhat satisfactory for the requirements. During the interval from

10 sec to 13 sec, where the sliding speed of the slider is reduced, the forward rolling velocity is also decreased compared to the period from 1 sec to 5 sec. This is an important result, which is used to control the rolling speed of the actual robot.

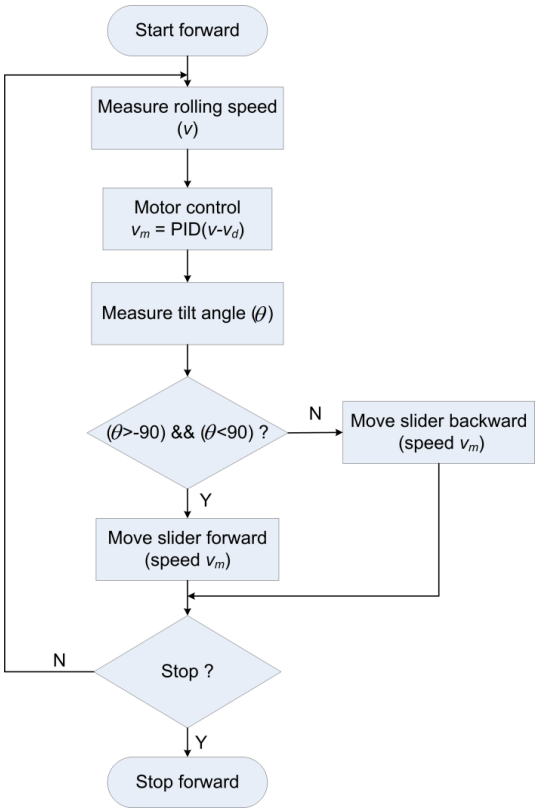

Figure 11. Control logic for forward rolling motion

Tilt angle (degree)	10	15	20	25
Jumping height (mm)	230	220	212	200
Jumping distance (mm)	180	200	210	218

Table 4. Jumping performance results of the robot

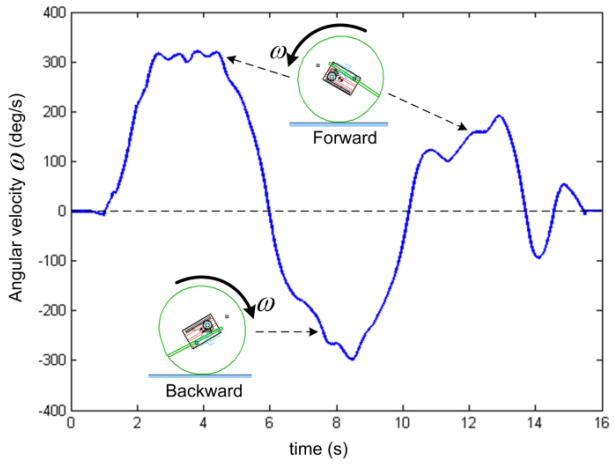

Figure 12. Rolling simulation of the robot

4. Conclusion

Design, analysis, and simulation of a novel jumping and rolling robot have been presented. The most outstanding feature is the minimum use of actuator. By using only one DC motor the robot is still able to perform both jumping and rolling locomotion. Simulation results show that the average rolling speed is up to 600 mm/sec, and so the equivalent travelling distance is about 2 km for one hour. In addition, the robot is able to jump up to nearly 1.3 times its diameter.

A tilt angle measurement method for rolling is also developed. The method is validated and applied for the control algorithm. Achievements of the robot can be summarized as follows. Firstly, using hybrid locomotion, rolling and jumping, the robot can adapt itself to various types of terrain. On a flat surface the rolling locomotion is utilized, while the jumping is useful for overcoming obstacles. This enhances both the manoeuvrability and the efficiency of the robot. Secondly, minimizing the number of actuators to one reduces the size, weight, complexity and power consumption of the robot. Energy efficiency is improved as a result.

5. Acknowledgements

This research was supported by Leading Foreign Research Institute Recruitment Program through the National Research Foundation of Korea (NRF) funded by the Ministry of Education, Science and Technology (MEST) (2011-00260).

6. References

[1] P. J. McKerrow, *Introduction to Robotics*, Addison-Wesley Pub, Boston, 1991.

[2] S. Bergbreiter, "Effective and efficient locomotion for millimeter-sized microrobots," in *Intelligent Robots and Systems (IROS 2008), 2008 IEEE/RSJ International Conference on*, pp. 4030-4035, 2008.

[3] R. M. Alexander, "Models and the scaling of energy costs for locomotion," *Journal of Experimental Biology*, vol. 208, pp. 1645-1652, 2005.

[4] M. Kovac, M. Schlegel, J.-C. Zufferey, and D. Floreano, "A miniature jumping robot with self-recovery capabilities," *Intelligent Robots and Systems, Proceedings of the 2009 IEEE/RSJ International Conference on, pp. 583-588*, St. Louis, MO, USA, 2009.

[5] M. Kovač, M. Schlegel, J.-C. Zufferey, and D. Floreano, "Steerable miniature jumping robot," *Autonomous Robots*, vol. 28, pp. 295-306, 2009.

[6] R. Armour et al., "Jumping robots: a biomimetic solution to locomotion across rough terrain," *Bioinspiration & Biomimetics*, vol. 2, p. S65, 2007.

[7] S. A. Stoeter, P. E. Rybski, M. Gini, and N. Papanikolopoulos, "Autonomous stair-hopping with Scout robots," in *Intelligent Robots and Systems, 2002 IEEE/RSJ International Conference on*, vol. 1, pp. 721-726, 2002.

[8] S. A. Stoeter and N. Papanikolopoulos, "Autonomous stair-climbing with miniature jumping robots," *Systems, Man, and Cybernetics, Part B: Cybernetics, IEEE Transactions on*, vol. 35, pp. 313-325, 2005.

[9] Y. Sugiyama, A. Shiotsu, M. Yamanaka, and S. Hirai, "Circular/Spherical Robots for Crawling and Jumping," in *Robotics and Automation (ICRA 2005), Proceedings of the 2005 IEEE International Conference on*, pp. 3595-3600, 2005.

[10] P. Ball, "Material witness: Rollobots," *Nat Mater*, vol. 6, pp. 261-261, 2007.

[11] J. Brackenbury, "Caterpillar kinematics," *Nature*, vol. 390, pp. 453-453, 1997.

[12] S. K. Karl. Real Wheel Animals - Part Two [Online]. Available: http://www.abc.net.au/science/articles/1999/08/09/42510.htm?site=science/greatmomentsinscience, Accessed on 25 Aug 2014.

[13] T. Ho and S. Lee, "Design and implementation of an SMA-actuated jumping robot," in *Intelligent Robots and Systems (IROS 2010), 2010 IEEE/RSJ International Conference on*, pp. 3530-3535, 2010.

[14] T. Ho and S. Lee, "A Shape Memory Alloy-Actuated Bio-inspired Mesoscale Jumping Robot," *International Journal of Advanced Robotic Systems*, vol. 9, pp. 1-8, 2012.

[15] M. Burrows, "Biomechanics: Froghopper insects leap to new heights," *Nature*, vol. 424, pp. 509-509, 2003.

[16] M. Burrows, "Morphology and action of the hind leg joints controlling jumping in froghopper insects," *J Exp Biol*, vol. 209, pp. 4622-4637, 2006.